Carbohydrate Polymers 98 (2013) 1011–1017

Contents lists available at SciVerse ScienceDirect

Carbohydrate Polymers

journal homepage: www.elsevier.com/locate/carbpol

Microencapsulation of *Lactobacillus helveticus* and *Lactobacillus delbrueckii* using alginate and gellan gum

Walfred Rosas-Flores, Emma Gloria Ramos-Ramírez, Juan Alfredo Salazar-Montoya *

Department of Biotechnology and Bioengineering, CINVESTAV-IPN, Av. IPN 2508, P.O. Box 14-740, CP 07360, México city, MEXICO

ARTICLE INFO

Article history:
Received 9 January 2013
Received in revised form 28 June 2013
Accepted 29 June 2013
Available online 8 July 2013

Keywords:
Activation energy
Emulsion
Microencapsulation
Internal ionic gelation
Sodium alginate
Low acylated gellan gum

ABSTRACT

Sodium alginate (SA) at 2% (w/v) and low acylated gellan gum (LAG) at 0.2% (w/v) were used to microencapsulate *Lactobacillus helveticus* and *Lactobacillus delbrueckii* spp *lactis* by employing the internal ionic gelation technique through water–oil emulsions at three different stirring rates: 480, 800 and 1200 rpm. The flow behavior of the biopolymer dispersions, the activation energy of the emulsion, the microencapsulation efficiency, the size distribution, the microcapsules morphology and the effect of the stirring rate on the culture viability were analyzed. All of the dispersions exhibited a non-Newtonian shear-thinning flow behavior because the apparent viscosity decreased in value when the shear rate was increased. The activation energy was calculated using the Arrhenius-like equation; the value obtained for the emulsion was 32.59 kJ/mol. It was observed that at 400 rpm, the microencapsulation efficiency was 92.83%, whereas at 800 and 1200 rpm, the stirring rates reduced the efficiency to 15.83% and 4.56%, respectively, evidencing the sensitivity of the microorganisms to the shear rate (13.36 and 20.05 s^{-1}). Both optical and scanning electron microscopy (SEM) showed spherical microcapsules with irregular topography due to the presence of holes on its surface. The obtained size distribution range was modified when the stirring rate was increased. At 400 rpm, bimodal behavior was observed in the range of 20–420 μm; at 800 and 1200 rpm, the behavior became unimodal and the range was from 20 to 200 μm and 20 to 160 μm, respectively.

1. Introduction

Microencapsulation is a powerful technique that allows a material to be packaged and protected from environmental and detrimental influences. A wide range of materials of biological interest has been microencapsulated, from small molecules and proteins to cells of bacterial, yeast and animal origins (Borgogna, Bellich, Zorzin, Lapasin, & Cesàro, 2010).

Currently, there are several methods of microencapsulation that have been classified as physical (Hatakeyama, Onishi, Endo, & Hatakeyama, 2007), physicochemical (Yáñez-Fernández, Ramos-Ramírez, & Salazar-Montoya, 2008), and chemical (Avadi et al., 2010). Internal ionic gelation, a physicochemical method, allows for the formation of spherically structured systems with sizes of less than 1000 μm by the interactions of cations and biopolymers with negative charge. These microsystems may contain a large variety of substances, active principles or microorganisms of industrial interest; additionally, internal ionic gelation is a simple, fast and low cost technique that also allows for the use of natural and inert polysaccharides as the core material (Ibarguren, Grosso, Apella, & Audisio, 2012).

Alginates are widely used in the food industry due to their viscosifying, non-toxic and gelling enhancing properties. Alginates are a group of polysaccharides produced by brown algae (*Laminaria hyperborea*, *Laminaria digitata*, *Laminaria japonica*) and bacteria (*Azotobacter vinelandii*, *Pseudomonas aeruginosa*). Chemically, alginate is an anionic linear copolymer of β-D-mannuronic acid (M) and α-L-guluronic acid (G) joined by links β 1-4 and is structured in blocks that can be homopolymeric (M or G) or heteropolymeric (MG) (Lee & Mooney, 2012). Alginate is synthesized as a biopolymer of mannuronic acid, which is subsequently transformed into guluronic acid by an enzymatic epimerization. The most important application of alginate in biotechnology is the ability to form stable gels through the ionic interaction between two adjacent G chains with Ca^{2+}, forming junction zones that stabilize the gel structure (Fabich et al., 2012).

Gellan gum is the most recent addition to the class of gelling agents commercially available for use in food. Gellan gum is an extracellular anionic heteropolysaccharide secreted by the bacterium *Sphingomonas elodea* and is composed of tetrasaccharide (1,3-β-D-glucose, 1,4-β-D-glucuronic acid, 1,4-β-D-glucose, 1,4-α-L-rhamnose) repeating units (González-Cuello, Ramos-Ramírez, Cruz-Orea, & Salazar-Montoya, 2012). Gellan gum is available in

* Corresponding author. Tel.: +52 55 57473800x4364; fax: +52 55 57473315.
E-mail address: jsalazar@cinvestav.mx (J.A. Salazar-Montoya).

0144-8617/$ – see front matter © 2013 Elsevier Ltd. All rights reserved.
http://dx.doi.org/10.1016/j.carbpol.2013.06.077

two forms: high (HAG) and low acylated (LAG). Low acylated gellan gum is formed by hydrolyzing the native gellan in a strong alkali solution at high temperatures to reduce the acyl groups (Okiror & Jones, 2012).

Gellan gum forms thermo-reversible gels at low concentrations (0.01–0.20%) in the presence of divalent cations (Ca^{2+} and Mg^{2+}); as a consequence, its usage has expanded and it is found in various products as a gelling agent that adds texture and stability (Yamamoto & Cunha, 2007). The gel characteristics depend mainly on the degree of substitution, pH, concentration and temperature. In the replaced form (HAG), elastic gels are produced, but in the non-replaced form (LAG), the formation of strong and brittle gels is favored (Abramovič & Klofutar, 2006).

The *Lactobacillus* genus, corresponding to lactic acid bacteria (LAB), plays a crucial role in the production of fermented dairy products as starters and adjunct/starters cultures; furthermore, the association of these microorganisms with health-promoting properties is of particular interest (Singh, Goswami, Singh, & Heller, 2009). Lactic acid bacteria (LAB) have an important role in food biotechnology because they have been used in the production of many fermented foods such as cheese and wine (Sohail, Turner, Coombes, & Bhandari, 2012). Microencapsulation can be carried out to reduce cell losses during food processing and storage, as well as to enhance the viability of LAB (Capela, Hay, & Shah, 2006). As the population of LAB may be affected by the microencapsulation process, it is important to ensure that the selected technique is compatible with the LAB organism (Pimentel-González, Campos-Montiel, Lobato-Calleros, Pedroza-Islas, & Vernon-Carter, 2009). Although there have been many studies about the microencapsulation of microorganism, there is almost no information concerning the use of anionic polysaccharides mixtures as encapsulating agents. In the present work, internal ionic gelation was used to microencapsulate *Lactobacillus helveticus* and *Lactobacillus delbrueckii* spp *lactis*, using a binary mixture of sodium alginate and low acylated gellan gum. The viscosity behavior of the polysaccharides, the emulsion activation energy, the size distribution of the microcapsules, the stirring rate and the effect of $CaCO_3$ on the microencapsulation efficiency and culture viability were determined.

2. Materials and methods

2.1. Materials

Sodium alginate (Satialgine), batch 6700322, was obtained from Cargill (USA). Low acylated gellan gum (Kelcogel F) was purchased from Kelco Biopolymers (USA). Calcium carbonate, batch 126K0064, and sorbitan monooleate (Span 80), batch 10K0911, were obtained from Sigma Aldrich (USA). Glacial acetic acid, batch K47476, was purchased from J.T. Baker (USA). The MRS agar (de Man, Rogosa, and Sharpe), batch VM059760, was obtained from Merck KGaA (Germany), and the MRS broth, batch 1146177, was purchased from Difco (USA). The canola oil, food grade, was purchased from Mazola (Aceites la Central, S.A. de C.V., México).

2.2. Methods

2.2.1. Rheological characterization of sodium alginate and low acylated gellan gum

The flow and viscosity behavior of the SA (2%), LAG (0.2%) and mixed system SA–LAG (2–0.2%) dispersions were determined at 25 °C with a LS100 low-stress rheometer (Paar-Physica, Germany) with torques of 1–5 mNm for SA, 1–3 mNm for LAG and 1–5 mNm for SA–LAG. A cylinder concentric DG1 geometry with 48 mm diameter and 36 mm length was used to generate shear rate and shear stresses ranging from 1.220×10^{-4} to $2.450 \times 10^{3}\ s^{-1}$ and from 6.37×10^{-3} to 6.37×10^{1} Pa, respectively. The data were adjusted to the Ostwald de Waele model (Eq. 1) and the cross model (Eq. 2) using the Curve Fitting Tool ver. 3.2.1 of Matlab® ver. 7.14.0.739.

$$\eta = K\dot{\gamma}^{n-1} \tag{1}$$

$$\eta = \eta_{\infty} + \frac{\eta_0 - \eta_{\infty}}{1 + (C\dot{\gamma}^{m})} \tag{2}$$

where n is the flow behavior index; K is the consistency coefficient; η is the apparent viscosity; η_{∞} is the limiting viscosity at infinite shear rate; η_0 is the limiting viscosity at zero shear rate; C is the cross time constant; m is the cross rate constant.

2.2.2. Viscous-flow activation energy of the emulsion

The activation energy was calculated using the Arrhenius-like equation (Eq. 3) by measuring the emulsion viscosity at different temperatures (25, 35, 45, and 55 °C). The viscosity was determined using a LS100 low-stress rheometer (Paar-Physica, Germany) with torques of 1–8 mNm for 25 °C, 1–8 mNm for 35 °C, 0.5–5 mNm for 45 °C, 0.1–4 mNm for 55 °C and 0.1–4 mNm for 65 °C. The cylinder concentric DG1 geometry with characteristics previously mentioned (Section 2.2.1) was used.

$$\eta = \eta_0 \exp\left(\frac{E_v}{RT}\right) \tag{3}$$

where η is the viscosity, η_0 is a pre-exponential constant associated with the nature of the liquid, R is the universal gas constant (8.314×10^{-3} kJ/mol K) and E_v is the viscous-flow activation energy. By plotting $\ln \eta$ vs. $1/T$, a straight line is obtained with a slope of E_v/R, which can be easily solved for E_v.

2.2.3. Bacterial strain and culture conditions

The pure lyophilized starter mixed culture LH100, commonly used in hard cheese production (containing *L. helveticus* and *L. delbrueckii* spp *lactis*), employed in this work was supplied by Distribuidora Alcatraz (México). The culture was transferred twice in MRS broth under aerobic conditions and maintained at 37 °C. After 24 h, the microorganisms were harvested by centrifugation at 9000 rpm and 4 °C for 10 min. The cell pellets were washed thrice and resuspended in a saline solution. Finally, the cells were enumerated by the spread plate method using MRS agar and were incubated at 37 °C for 48 h. The final cell concentration was adjusted to 10^9 CFU/mL.

2.2.4. Microencapsulation

The microcapsules were prepared through internal ionic gelation; this technique is based on the formation of a water–oil emulsion. The aqueous phase was prepared mixing 1 mL of the cell suspension (MOs, 10^9 CFU) with 99 mL of the SA–LAG dispersion (2% and 0.2% of SA and LAG, respectively, and previously autoclaved at 121 °C for 15 min), and 0.4 g calcium carbonate was added as a Ca^{2+} donor. The MOs-SA–LAG dispersion was added to the oily phase (200 mL of commercial canola oil premixed with 5 mL of Span 80) at constant agitation (400, 800 and 1200 rpm) in a stirring plate (RCT Basic, IKAMAG S1 IKA, USA) to begin the emulsion process. 40 mL of canola oil containing glacial acetic acid was incorporated to start the internal ionic gelation process. The system was agitated for 20 min. The microcapsules were harvested by centrifugation at 3000 rpm for 5 min, and the pellets were washed thrice with Phosphate Buffered Saline (PBS) solution to remove the oil residues. Finally, the microcapsules were stored under refrigeration at 4 °C until further analysis.

2.2.5. Determination of the morphology of the microcapsules by optical microscopy

To determine the morphology and diameter of the microcapsules, an Olympus Model IX50 (Olympus, Japan) microscope was used. The diameters were determined from the micrographs of the observation fields using integrated software (Image Pro Express ver. 4.0). Once the diameters were obtained, the frequency curve and particle size distribution were obtained at intervals of 20 μm; from the obtained results, the average, standard deviation and least significant differences were determined.

2.2.6. Determination of the morphology of the microcapsules by scanning electron microscopy

The microcapsules were fixed with 2.5% glutaraldehyde for 1 h and were then washed thrice with a PBS solution. The samples were dehydrated using an ethanol gradient at 50, 60, 70, 80, 90, and 100% and were maintained for 15 min in each concentration. Then, the samples were dried at the critical point in the presence of carbon dioxide using a Samdri-780 dehydrator (Tousimis, USA). Subsequently, a gold coating was deposited by a DESK II gold sputter machine (Denton Vacuum, USA) over 1 min. Finally, the microcapsules were observed using a scanning electron microscope (JSM-35C, JEOL, Germany). The glutaraldehyde was used to fix the microorganism contained in the microcapsule structure to prevent bacteria loss; the microcapsules are fixed with double sided adhesive tape commonly used in MEB observations. This technique has been used and previously reported by Yáñez-Fernández et al. (2008).

2.2.7. Microencapsulation efficiency and culture viability

To evaluate the microencapsulation efficiency, the microorganisms were released according to the method of Zou et al. (2012) with some modifications. The microcapsules (1 g) were mixed with phosphate buffer (pH 7, 0.1 M) and homogenized for 60 s at 15,000 rpm using a high-speed homogenizer (Ultra-Turrax, model T25 D S1, IKA® Werke Gmbh & Co. KG, Germany), and 1 mL of the homogenized solution was 10-fold diluted into peptone water (previously cleaved 121 °C, 15 min); thereafter, 0.1 mL aliquots of the dilutions were plated in triplicate onto MRS agar. All of the plates were incubated at 37 °C for 48 h before enumeration. This technique has been demonstrated to be friendly with the microencapsulated microorganisms, since the stresses generated impact directly on the structure of microcapsules and no on bacteria cells. The homogenization speed does not decrease the viability of the microorganism, and this technique has been used in some studies as reported by Chávarri et al. (2010), Nag, Han, and Singh (2011) and Zou et al. (2012). The microencapsulation efficiency was determined using Eq. (4).

$$E_m = \frac{C_f}{C_i} \times 100 \quad (4)$$

where C_i is the number of viable bacteria cells before the microencapsulation and C_f corresponds to the number of viable microorganisms released from the microcapsules. The results were analyzed by ANOVA with $p < 0.05$ to determine the least significant differences using Minitab software ver. 15.1.

3. Results and discussion

3.1. Viscosity and behavior of SA, LAG and SA–LAG dispersions

Fig. 1 shows the apparent viscosity (η) of the three aqueous dispersions containing sodium alginate (SA, 2% w/v), low acylated gellan gum (LAG, 0.2% w/v) and the SA–LAG mixed system (2% and 0.2% w/v, respectively) as a function of the shear rate (γ) at 25 °C. All three viscosity curves exhibited shear-thinning behavior where

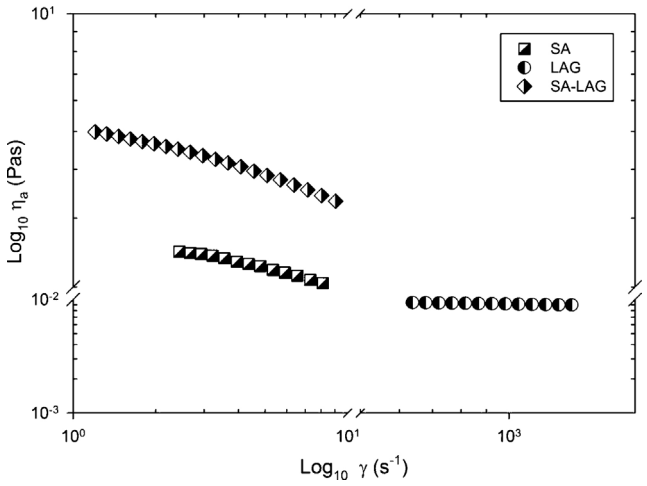

Fig. 1. The viscosity behavior vs. the shear rate of sodium alginate (SA), low acylated gellan gum (LAG) and mixed sodium alginate–low acylated gellan gum (SA–LAG) dispersions.

the apparent viscosity decreased slightly as the shear rate increased and the flow behavior index was less than unity ($n < 1$); this flow behavior has been already reported by Kayacier and Dogan (2006) for alginate and González-Cuello et al. (2012) for gellan gum dispersions. The average viscosity obtained was 2.122 ± 0.256 Pa s for SA, 0.009 ± 0.000 Pa s for LAG and 4.237 ± 0.523 Pa s for the SA–LAG mixed system. The least significant differences (Fisher method, 95% confidence) were founded between all three values. The differences between the SA and LAG systems can be explained as the dependence of the apparent viscosity on the concentration of polysaccharide and shear rate; the conformation of the molecules also had an effect. The difference between the individual systems (SA and LAG) and the mixed system (SA–LAG) may be due to a synergistic effect among the polysaccharides; this effect can be observed by the increase in the viscosity value, which was 2 times with respect to SA and 466 times with respect to LAG. However, there is a lack of information about sodium alginate and low acyl gellan gum interaction at molecular level, only a few studies has been published on this topic, due to the complexity of the experimental validation. Panouillé and Larreta-Garde (2009) studied the synergism between sodium alginate and gelatin from rheological point of view and concluded that the mixed system could be stabilized through electrostatic interaction between charges of biopolymers and Ca^{2+} cations; in this sense, the synergistic effect may occur through the hydrogen bonding between SA and LAG, and thus resulting in a more structured system than its individual form.

In shear-thinning behavior, three distinct regions may be exhibited: a lower Newtonian region where the apparent viscosity (limiting viscosity at zero shear rate, η_0) is constant over a limited shear rate range, a middle region where the apparent viscosity (η) is decreasing as the shear rate is increased, and an upper Newtonian region where the apparent viscosity (limiting viscosity at infinite shear rate, η_∞) is constant with changing shear rates. The rearrangement in the conformation of the polysaccharides molecules in the dispersion due to shearing may be the origin of the three regions in shear-thinning behavior. The Ostwald de Waele and cross models were used to fit data obtained from the flow curves and are presented in Table 1; all of the adjustments were acceptable because the correlations coefficients ranged between 0.970 and 1. As seen in Table 1 from the Ostwald de Waele model, the highest value for K was obtained for the mixed system (SA–LAG) and the lowest was obtained for LAG dispersion, with an intermediate value for SA; the consistency coefficient (K) may be considered to be the viscosity value when the shear rate is equal

Table 1
The Ostwald de Waele and cross parameters obtained from flow curves fit.

Sample	Ostwald de Waele			Cross				
	n (–)	K (Pa s^n)	R^2 (–)	η_0 (Pa s)	η_∞ (Pa s)	C (s^m)	m (–)	R^2
SA	0.809^a	3.003^a	0.980	2.788^a	0.698^a	0.078^a	0.936^a	0.999
LAG	0.932^b	0.015^b	0.998	0.250^b	0.008^b	0.801^b	0.890^a	0.988
SA–LAG	0.805^a	5.276^c	0.987	6.155^c	0.104^c	0.213^c	0.646^b	0.999

SA, sodium alginate; LAG, low acylated gellan gum; SA–LAG, sodium alginate–low acylated gellan gum mixture; n, flow behavior index; K, consistency coefficient; R^2, correlation coefficient; η_∞, limiting viscosity at infinite shear rate; η_0, limiting viscosity at zero shear rate; C, cross time constant; n_c, cross rate constant; (–), dimensionless. In each column different superscript letters denoted statistically significative differences (Fisher, $p < 0.05$).

to 1 ($\dot{\gamma} = 1$). Moreover, the flow behavior index (n) obtained for all three dispersions shows the pseudoplasticity of the dispersions because greater departures from unity show more pronounced shear-thinning behavior. In the cross model, the cross time constant (C, s^m) can be considered as the characteristic time and generally gives an order of magnitude of the critical shear rate, which marks the end of the limiting viscosity at the zero shear rate plateau and the onset where shear-thinning behavior begins. According to the above and the fit obtained (Table 1), shear-thinning behavior begins at 12.851 s, 1.124 s and 4.688 s for SA, LAG and SA–LAG, respectively. K, n, and C are important parameters because they provide useful information for process design at the industrial level.

3.2. Activation energy

The emulsification process has an important role in microcapsule formation because it may be considered to be the starting point of many microencapsulation techniques such as coacervation, spray drying and internal ionic gelation. Because emulsion formation involves shearing, it is important to understand concepts such as the activation energy related to the system viscosity. In fluids, the activation energy may be thought of as the barrier to overcome to allow molecules to move; this barrier is created by the resistance of the surrounding building units. Fig. 2A shows the temperature dependence of the emulsion viscosity; the data values were obtained by analyzing the flow behavior of the emulsion at 25, 35, 45 and 55 °C (298.15, 308.15, 318.15 and 328.15 K, respectively), and the curves resulting were fitted to a Newtonian model with correlation coefficients greater than 0.990. It can be seen that temperature effects reduce the viscosity values by 70%, from 152 mPa s at 25 °C (298.15 K) to 45 mPa s at 55 °C (328.15 K). The decrease in viscosity can be attributed to the increases in the intermolecular spaces as a consequence of thermal expansion when the temperature is increased (Xiao, Tong, & Lim, 2012). Fig. 2B shows the relationship of ln η vs. $1/T$; from the adjusted data, the activation energy was calculated as 32.59 kJ/mol. This value approximated the value obtained by Ibanoglu (2002), who reported activation energies between 25.189 kJ/mol and 31.417 kJ/mol in the temperature range of 22–45 °C in an emulsion system. According to Karaman, Yilmaz, Dogan, Yetim, and Kayacier (2011), high activation energy values may indicate that the dynamical shear properties of the emulsion are highly temperature dependent; and, high values for the activation energy suggest that a dense and structured matrix is formed around the active principle, protecting it from thermal stress (Muñoz-Celaya et al., 2012). In present study, activation energy was not calculated as a function of temperatures. We calculated emulsion viscosity at different temperatures to determinate activation energy through Arrhenius type equation (Eq. 3).

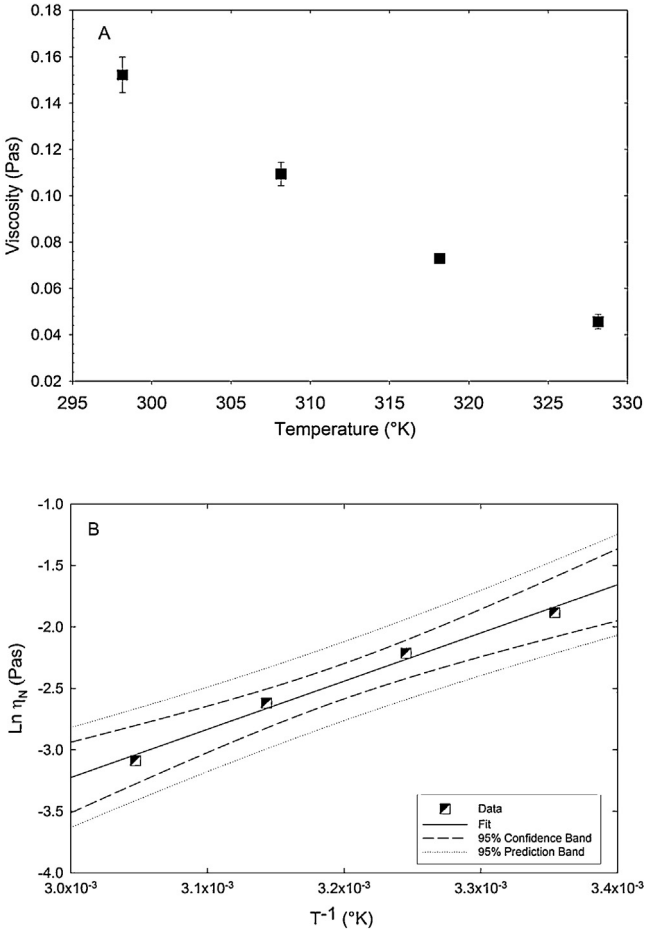

Fig. 2. The activation energy calculation: (A) the viscosity behavior vs. the temperature of the emulsion and (B) ln η_N vs. $1/T$.

3.3. Size distribution and optical and scanning electron microscopy of microcapsules

3.3.1. Size distribution

The size distribution of the microcapsules prepared by the emulsion-based methodology is highly correlated with the internal phase viscosity and other factors such as the pH, temperature and stirring rate. This work investigated the effect of three different stirring rates (400, 800, and 1200 rpm) on the size distribution at constant viscosity (same concentration), pH (4.5) and temperature (25 °C). Fig. 3A–C shows the number of microcapsules versus particle size intervals obtained at 400, 800, and 1200 rpm. The figures show that at 400 rpm, a bimodal behavior was obtained with two peaks, one at 20–40 μm with 34% frequency and the other at 400–420 μm with 5% frequency. According to Heidebach, Först, and Kulozik (2009), this variation in the size distribution can be attributed to the high viscosity ratio between the dispersed and the continuous phase, which hinders the severance of the microdroplets in the dispersed phase and allows for large microcapsules to often be obtained. This effect was diminished at higher stirring rates, as at 800 rpm, the maximum frequency obtained was 24% in the 100–120 μm interval (Fig. 3B) and unimodal behavior was

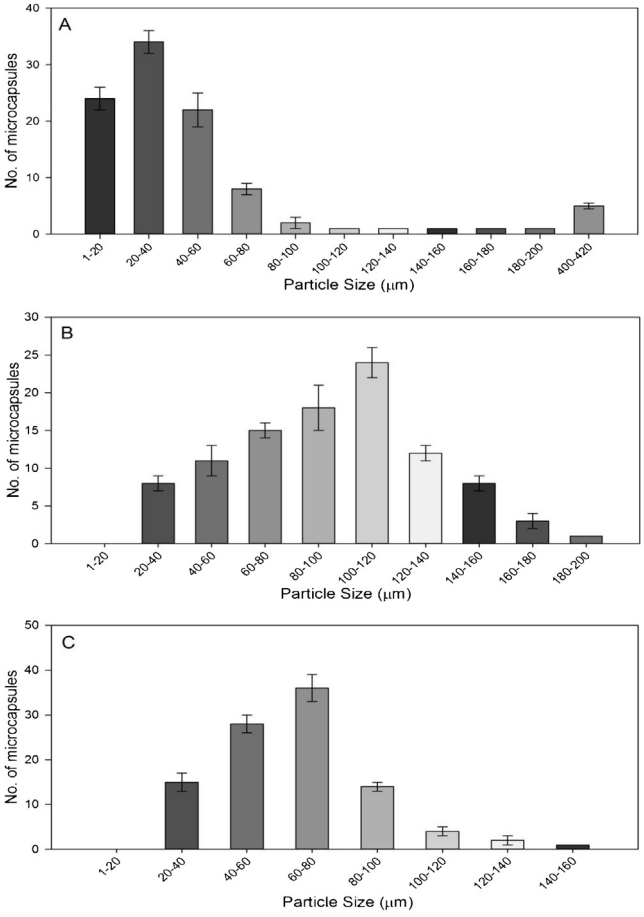

Fig. 3. The size distributions of the microcapsules obtained at different stirring rates: (A) 400 rpm, (B) 800 rpm, and (C) 1200 rpm.

observed with particle sizes between 20 and 200 μm. When the stirring rate was increased to 1200 rpm (Fig. 3C), the shortest interval was found with particle sizes between 20 and 160 μm. This was 25% below the interval obtained with 800 rpm and 165% below the interval obtained with 400 rpm; the maximum frequency obtained was 36% in the 60–80 μm interval. Microcapsule size distributions have been reported by many authors, but few have reported the optimum microcapsule size as the optimum depends on many factors; for example, in food applications, where the efficiency-sensory relation could be the most important factor, an optimum range of 100–200 μm has been proposed for many applications (Nag et al., 2011). The size distribution obtained in this work clearly produces the above range at stirring rates of 800 and 1200 rpm.

3.3.2. Optical and scanning electron microscopy

The surface morphology of the microcapsules was analyzed by optical and scanning electron microscopy. Fig. 4 shows micrographs of the microcapsules prepared at 400 rpm (A), 800 rpm (B) and 1200 rpm (C). The figure shows that an inverse effect was observed, that is, when the stirring rate was increased, the size distribution decreased; this behavior agrees with what was reported by Ma et al. (2009) in the microencapsulation of tamoxifen using acacia gum and gelatin through complex coacervation (an emulsion based-method). It can be seen that the morphology of the microcapsules obtained with SA at 2% and LAG at 0.2%, using calcium carbonate as a Ca^{2+} donor, are spherical in shape with regular surfaces without the presence of peaks or deformations.

Fig. 5 shows a series of micrographs obtained by scanning electron microscopy for microcapsules prepared at 400 rpm. The SEM

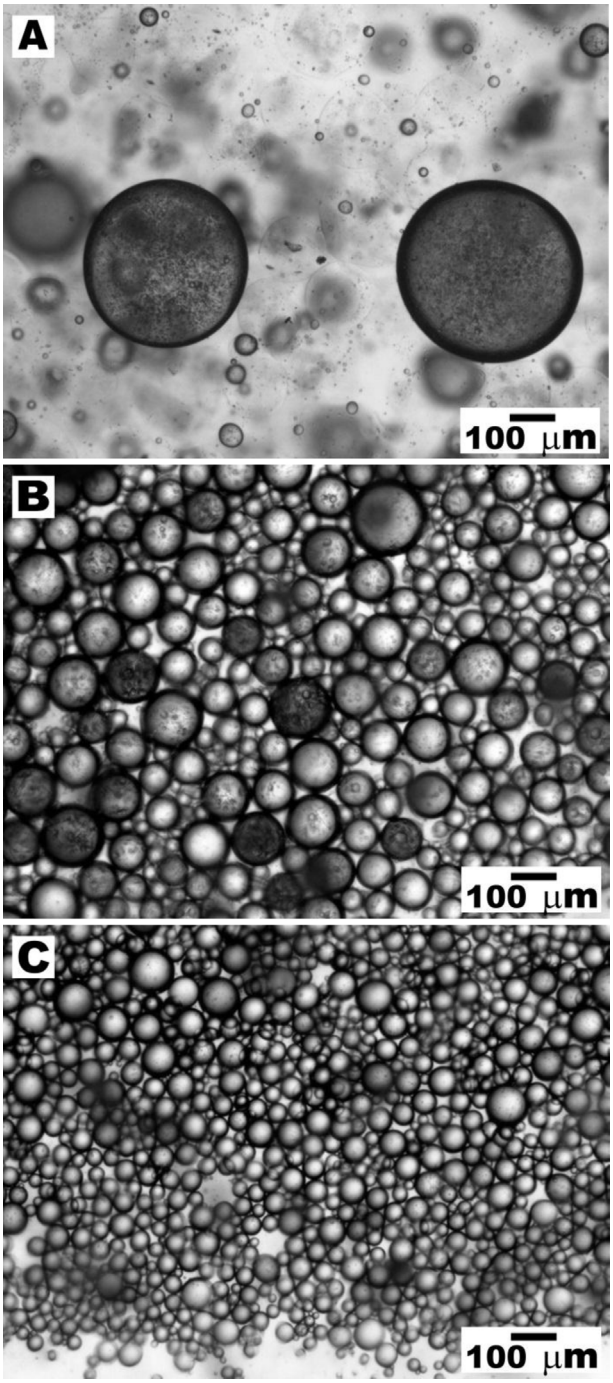

Fig. 4. The optical micrographs at 4× of the microcapsules prepared using different stirring rates: (A) 400 rpm, (B) 800 rpm, and (C) 1200 rpm.

revealed spherical morphologies with irregular surface topography (Fig. 5A and B), which can be attributed to the loss of water during the microcapsules drying process for SEM analysis. Although many microcapsules were dispersed, clusters of different numbers of microcapsules were observed; this is most likely due to the cohesive nature of the biopolymers (SA and LAG). At higher magnifications of 4000× (Fig. 5C) and 6000× (Fig. 5D), holes can be observed on the microcapsule surface; these holes could allow for the free diffusion of nutrients (from the outside to the inside of the microcapsule) and the metabolism products of the microencapsulated microorganisms (from the inside to the outside). However, these holes may be caused by the diffusion of functionally active

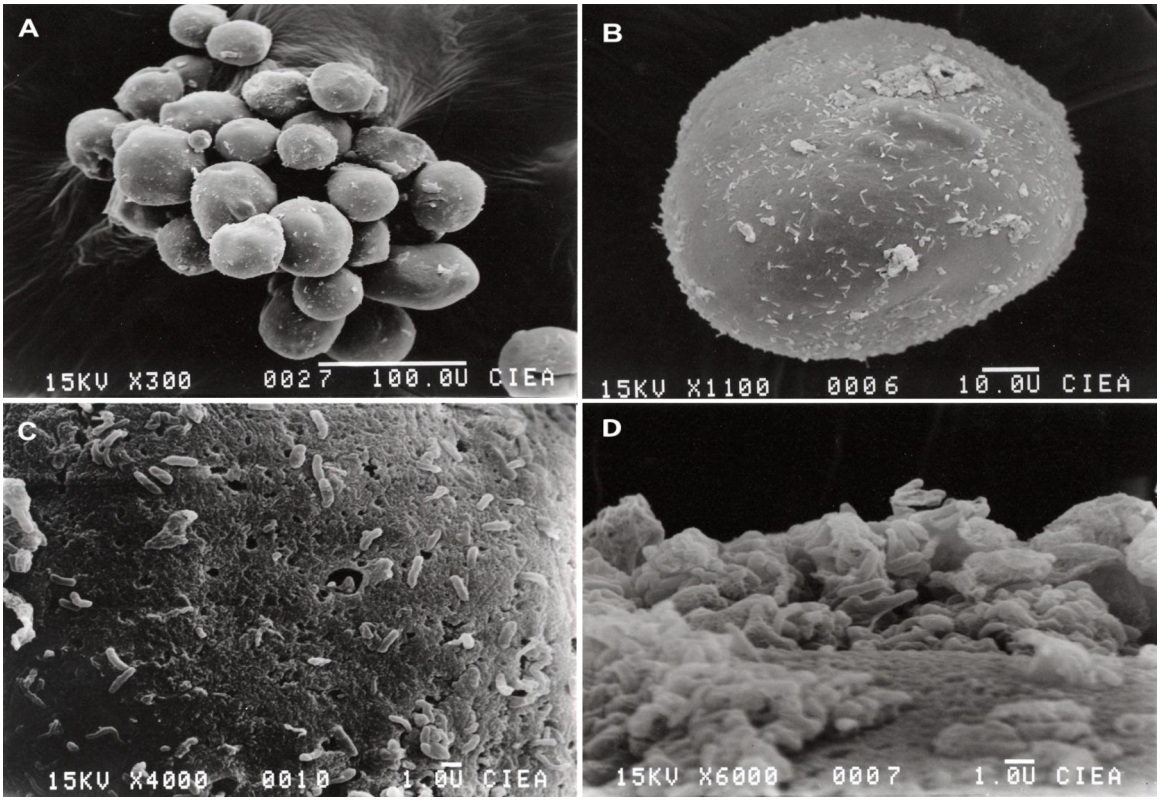

Fig. 5. The scanning electron micrographs of the microcapsules obtained at 400 rpm with different magnifications: (A) 300×, (B) 1100×, (C) 4000×, and (D) 6000×.

microorganisms clusters (biomass diffusion), and these clusters can cause the rupture of the matrix that can be observed as holes. The number of holes increased with the formation time of the microcapsules (Quirós, Rendueles, García, & Díaz, 1995).

3.4. Viability of the microencapsulated microorganisms

The culture viability was determined by enumerating the microorganisms (CFU) at three different stages of the microencapsulation process to observe any detrimental effects caused by the technique methodology. The initial count (Ci, black bar, Fig. 6) corresponds to the number of microorganism (MOs) added to the SA–LAG dispersion (aqueous phase). No negative effects on the culture viability were caused by the addition of $CaCO_3$ (Ca^{2+} donor) to the MOs-SA–LAG dispersion as shown in Fig. 6, as no significant differences exist between the Ci count and the count before the microencapsulation process (gray bars). Thereafter, emulsions were formed by mixing the MOs-SA–LAG dispersion and canola oil premixed with Span 80 at 480, 800 and 1200 rpm, followed by the addition of acetic acid to induce the gelation process. Two counts were determined; the first count was in the supernatant obtained after microcapsules harvesting process to determine if the MOs were released and therefore not microencapsulated. However, no CFU were observed in dilutions from 10^{-1} to 10^{-8}, suggesting that all of the active MOs were microencapsulated. The second count was determined after the microcapsules were harvested; the MOs were released from the microcapsules and the CFU was ascertained to determine the efficiency and the effect of the stirring rate on the culture viability. No negative effect was observed at 400 rpm (white bar, Fig. 6), as there was no significant difference ($p < 0.05$) between the CFU values obtained before and after microencapsulation process; the calculated efficiency was 92.83%. However, when the stirring rate increases, a negative effect on the culture viability after microencapsulation was observed, as the efficiency decreases drastically with respect to the value obtained at 400 rpm; at 800 rpm, the calculated efficiency was 15.83% with respect to the initial count (77.00% below the value obtained at 400 rpm) and the CFU values before and after the microencapsulation process were significantly different ($p < 0.05$). At 1200 rpm, the negative effect was higher than that obtained at 800 rpm because efficiency was 4.56%, representing a decrease of 88.27% and 11.27% with respect to the values obtained at 400 rpm and 800 rpm, respectively. The final count at 1200 rpm was significantly different from the initial count, but no difference was found with respect to the

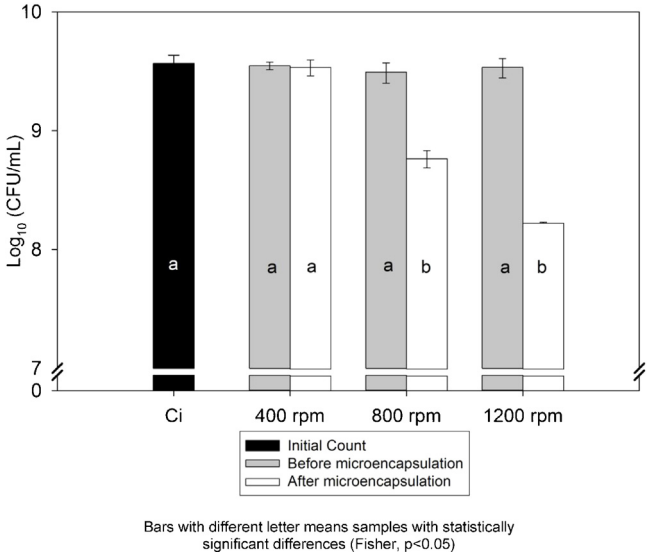

Fig. 6. The microorganism counts obtained at different stages of the microencapsulation process.

value obtained at 800 rpm ($p < 0.05$). In summary, by increasing the stirring rate 3-fold, from 400 rpm to 1200 rpm, the efficiency decreased by 88.27%; this effect can be attributed to the sensitivity of microorganism to the changes in the generated shear rate (6.68 s^{-1}, 13.36 s^{-1} and 20.05 s^{-1} at 400, 800, and 1200 rpm, respectively). *L. helveticus* is one of the main microbial species that have been reported as a probiotic (Ranadheera, Baines, & Adams, 2010), and to provide health benefits, probiotic dose levels have been recommended at a minimum of 10^6–10^7 CFU/g per day (Burgain, Gaiani, Linder, & Scher, 2011). The CFU levels obtained after the microencapsulation process at all three stirring rates (Fig. 6) are within the recommended value.

4. Conclusions

Internal ionic gelation using sodium alginate and low acylated gellan gum produced size distributions that are within those reported for optimal food applications. The size distribution–viability relationship has a major role in the selection of the stirring rate for microencapsulation processes through internal ionic gelation. The stirring rate has a major role on the microencapsulation efficiency of *L. helveticus* and *L. delbrueckii* spp *lactis* because it drastically affects the culture viability as it was observed; however, this reduction could be acceptable inasmuch as all the CFU counts after the microencapsulation process demonstrated values that are within the reported as the minimum dose levels per day. Currently it has been reported, a great loss of microorganisms in cheeses production during manufacture process (Ortakci, Broadbent, McManus, & McMahon, 2012), in this sense it is important protect the microorganisms against deleterious conditions; also it has been reported probiotic activity of *L. helveticus* by the numerous benefits to human health. The authors are considering future studies where the viability of microorganisms microencapsulates, will be measured in vitro at different pH.

Acknowledgments

The authors are grateful for the scholarship granted to Walfred Rosas-Flores by CONACYT during the development of this work, to Miguel Marquez for his technical support and Ma. de Lourdes Rojas for her support in obtaining the micrographs.

References

Abramovič, H., & Klofutar, C. (2006). Water adsorption isotherms of some gellan gum samples. *Journal of Food Engineering*, *77*(3), 514–520. http://dx.doi.org/10.1016/j.jfoodeng.2005.06.064

Avadi, M. R., Sadeghi, A. M., Mohammadpour, N., Abedin, S., Atyabi, F., Dinarvand, R., et al. (2010). Preparation and characterization of insulin nanoparticles using chitosan and Arabic gum with ionic gelation method. *Nanomedicine*, *6*(1), 58–63. http://dx.doi.org/10.1016/j.nano.2009.04.007

Borgogna, M., Bellich, B., Zorzin, L., Lapasin, R., & Cesàro, A. (2010). Food microencapsulation of bioactive compounds: Rheological and thermal characterisation of non-conventional gelling system. *Food Chemistry*, *122*(2), 416–423. http://dx.doi.org/10.1016/j.foodchem.2009.07.043

Burgain, J., Gaiani, C., Linder, M., & Scher, J. (2011). Encapsulation of probiotic living cells: From laboratory scale to industrial applications. *Journal of Food Engineering*, *104*(4), 467–483. http://dx.doi.org/10.1016/j.jfoodeng.2010.12.031

Capela, P., Hay, T. K. C., & Shah, N. P. (2006). Effect of cryoprotectants, prebiotics and microencapsulation on survival of probiotic organisms in yoghurt and freeze-dried yoghurt. *Food Research International*, *39*(2), 203–211. http://dx.doi.org/10.1016/j.foodres.2005.07.007

Chávarri, M., Marañón, I., Ares, R., Ibáñez, F. C., Marzo, F., & Villarán, M. C. (2010). Microencapsulation of a probiotic and prebiotic in alginate-chitosan capsules improves survival in simulated gastro-intestinal conditions. *International Journal of Food Microbiology*, *142*(1/2), 185–189. http://dx.doi.org/10.1016/j.ijfoodmicro.2010.06.022

Fabich, H. T., Vogt, S. J., Sherick, M. L., Seymour, J. D., Brown, J. R., Franklin, M. J., et al. (2012). Microbial and algal alginate gelation characterized by magnetic resonance. *Journal of Biotechnology*, *161*(3), 320–327. http://dx.doi.org/10.1016/j.jbiotec.2012.04.016

González-Cuello, R. E., Ramos-Ramírez, E. G., Cruz-Orea, A., & Salazar-Montoya, J. A. (2012). Rheological characterization and activation energy values of binary mixtures of gellan. *European Food Research and Technology*, *234*(2), 305–313. http://dx.doi.org/10.1007/s00217-011-1626-2

Hatakeyama, H., Onishi, T., Endo, T., & Hatakeyama, T. (2007). Gelation of chemically cross-linked methylcellulose studied by DSC and AFM. *Carbohydrate Polymers*, *69*(4), 792–798. http://dx.doi.org/10.1016/j.carbpol.2007.02.022

Heidebach, T., Först, P., & Kulozik, U. (2009). Microencapsulation of probiotic cells by means of rennet-gelation of milk proteins. *Food Hydrocolloids*, *23*(7), 1670–1677. http://dx.doi.org/10.1016/j.foodhyd.2009.01.006

Ibanoglu, E. (2002). Rheological behaviour of whey protein stabilized emulsions in the presence of gum arabic. *Journal of Food Engineering*, *52*(3), 273–277. http://dx.doi.org/10.1016/S0260-8774(01)00115-7

Ibarguren, C., Grosso, C. R. F., Apella, M. C., & Audisio, M. C. (2012). Anti-Listeria monocytogenes activity of enterocins microencapsulated by ionic gelation. *Food Hydrocolloids*, *29*(1), 21–26. http://dx.doi.org/10.1016/j.foodhyd.2012.01.017

Karaman, S., Yilmaz, M. T., Dogan, M., Yetim, H., & Kayacier, A. (2011). Dynamic oscillatory shear properties of O/W model system meat emulsions: Linear viscoelastic analysis for effect of temperature and oil concentration on protein network formation. *Journal of Food Engineering*, *107*(2), 241–252. http://dx.doi.org/10.1016/j.jfoodeng.2011.06.016

Kayacier, A., & Dogan, M. (2006). Rheological properties of some gums-salep mixed solutions. *Journal of Food Engineering*, *72*(3), 261–265. http://dx.doi.org/10.1016/j.jfoodeng.2004.12.005

Lee, K. Y., & Mooney, D. J. (2012). Alginate: Properties and biomedical applications. *Progress in Polymer Science*, *37*(1), 106–126. http://dx.doi.org/10.1016/j.progpolymsci.2011.06.003

Ma, Z. H., Yu, D. G., Branford-White, C. J., Nie, H. L., Fan, Z. X., & Zhu, L. M. (2009). Microencapsulation of tamoxifen: Application to cotton fabric. *Colloids and Surfaces B: Biointerfaces*, *69*(1), 85–90. http://dx.doi.org/10.1016/j.colsurfb.2008.11.005

Muñoz-Celaya, A. L., Ortiz-García, M., Vernon-Carter, E. J., Jauregui-Rincón, J., Galindo, E., & Serrano-Carreón, L. (2012). Spray-drying microencapsulation of *Trichoderma harzianum* conidias in carbohydrate polymers matrices. *Carbohydrate Polymers*, *88*(4), 1141–1148. http://dx.doi.org/10.1016/j.carbpol.2011.12.030

Nag, A., Han, K.-S., & Singh, H. (2011). Microencapsulation of probiotic bacteria using pH-induced gelation of sodium caseinate and gellan gum. *International Dairy Journal*, *21*(4), 247–253. http://dx.doi.org/10.1016/j.idairyj.2010.11.002

Okiror, G. P., & Jones, C. L. (2012). Effect of temperature on the dielectric properties of low acyl gellan gel. *Journal of Food Engineering*, *113*(1), 151–155. http://dx.doi.org/10.1016/j.jfoodeng.2012.04.011

Ortakci, F., Broadbent, J. R., McManus, W. R., & McMahon, D. J. (2012). Survival of microencapsulated probiotic *Lactobacillus paracasei* LBC-1e during manufacture of Mozzarella cheese and simulated gastric digestion. *Journal of Dairy Science*, *95*(11), 6274–6281. http://dx.doi.org/10.3168/jds.2012-5476

Panouillé, M., & Larreta-Garde, V. (2009). Gelation behavior of gelatin and alginate mixtures. *Food Hydrocolloids*, *23*(4), 1074–1080. http://dx.doi.org/10.1016/j.foodhyd.2008.06.011

Pimentel-González, D. J., Campos-Montiel, R. G., Lobato-Calleros, C., Pedroza-Islas, R., & Vernon-Carter, E. J. (2009). Encapsulation of *Lactobacillus rhamnosus* in double emulsions formulated with sweet whey as emulsifier and survival in simulated gastrointestinal conditions. *Food Research International*, *42*(2), 292–297. http://dx.doi.org/10.1016/j.foodres.2008.12.002

Quirós, C., Rendueles, M., García, L. A., & Díaz, M. (1995). Diffusion of microorganisms in calcium alginate beads. *Biotechnology Techniques*, *9*(11), 809–814. http://dx.doi.org/10.1007/bf00159406

Ranadheera, R. D. C. S., Baines, S. K., & Adams, M. C. (2010). Importance of food in probiotic efficacy. *Food Research International*, *43*(1), 1–7. http://dx.doi.org/10.1016/j.foodres.2009.09.009

Singh, S., Goswami, P., Singh, R., & Heller, K. J. (2009). Application of molecular identification tools for *Lactobacillus*, with a focus on discrimination between closely related species: A review. *LWT – Food Science and Technology*, *42*(2), 448–457. http://dx.doi.org/10.1016/j.lwt.2008.05.019

Sohail, A., Turner, M. S., Coombes, A., & Bhandari, B. (2012). The viability of *Lactobacillus rhamnosus* GG and *Lactobacillus acidophilus* NCFM following double encapsulation in alginate and maltodextrin. *Food and Bioprocess Technology*, *1-7* http://dx.doi.org/10.1007/s11947-012-0938-y

Xiao, Q., Tong, Q., & Lim, L.-T. (2012). Pullulan-sodium alginate based edible films: Rheological properties of film forming solutions. *Carbohydrate Polymers*, *87*(2), 1689–1695. http://dx.doi.org/10.1016/j.carbpol.2011.09.077

Yamamoto, F., & Cunha, R. L. (2007). Acid gelation of gellan: Effect of final pH and heat treatment conditions. *Carbohydrate Polymers*, *68*(3), 517–527. http://dx.doi.org/10.1016/j.carbpol.2006.11.009

Yáñez-Fernández, J., Ramos-Ramírez, E., & Salazar-Montoya, J. (2008). Rheological characterization of dispersions and emulsions used in the preparation of microcapsules obtained by interfacial polymerization containing *Lactobacillus* sp. *European Food Research and Technology*, *226*(5), 957–966. http://dx.doi.org/10.1007/s00217-007-0617-9

Zou, Q., Liu, X., Zhao, J., Tian, F., Zhang, H.-p., Zhang, H., et al. (2012). Microencapsulation of *Bifidobacterium bifidum* F-35 in whey protein-based microcapsules by transglutaminase-induced gelation. *Journal of Food Science*, *77*(5), M270–M277. http://dx.doi.org/10.1111/j.1750-3841.2012.02673.x